Machine Learning Techniques for Energy Reconstruction in JUNO experiment

Arsenii Gavrikov, Fedor Ratnikov on behalf of the JUNO collaboration

E-mail: gavrikov.997755@gmail.com

Introduction

1. Jiangmen Underground Neutrino Observatory (JUNO):
   - multipurpose experiment;
   - 53 km away from 8 reactor cores in China;
   - ~600-meter deep underground;
   - data taking expected in ~2023.
2. The main goals of JUNO:
   - neutrino mass ordering (3σ in 6 years);
   - precise measure of oscillation parameters $\sin^2\theta_{12}, \Delta m^2_{21}, \Delta m^2_{31}$.
3. The Central Detector:
   - detection channel: $\bar{\nu}_e + p \to e^+ + n$;
   - deposited energy converts to optical light;
   - the largest liquid scintillator detector: 20 kt;
   - 77.9% photo-coverage: 18k 20”, 26k 3” photo-multiplier tubes (PMTs).

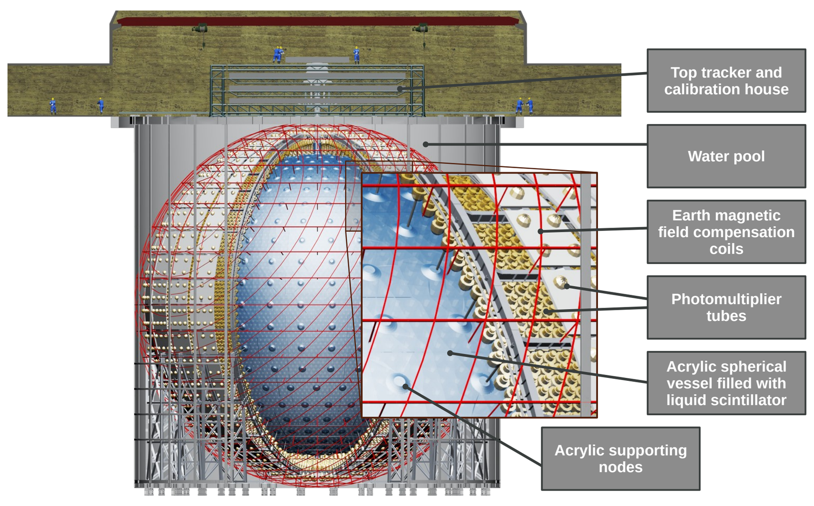

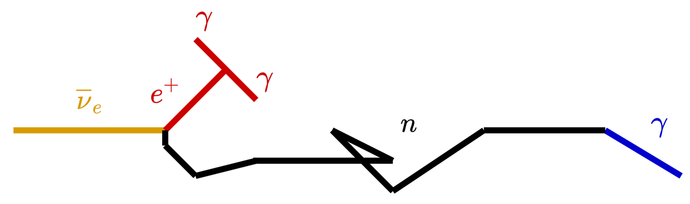

Problem statement

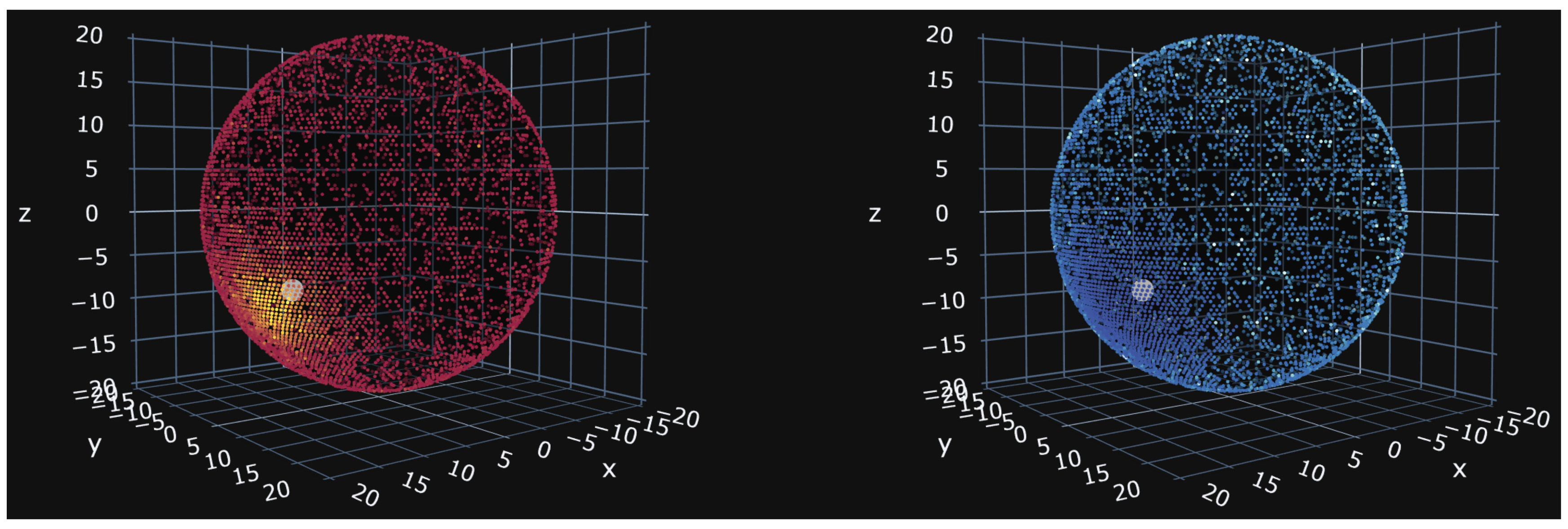

Example of an event seen by 20” PMTs for a positron of 6.165 MeV deposited energy. The color represents the accumulated charge in PMTs (left) and PMT activation time (right). The gray sphere: the primary vertex.

Avaliable information:
- Charge at each PMT;
- First Hit Time (FHT) at each PMT;
- PMT position.

We want to provide:

Deposited energy E_{dep} with resolution 3% @ 1 MeV.

Data description

To train model and to evaluate model performance we prepared two datasets generated by the full detector Monte Carlo method using the official JUNO software:

1. **Training dataset:**
   - 5 million positron events;
   - uniformly distributed in kinetic energy E_{kin};
   - uniformly spread in the volume of the central detector;
   - $E_{\text{kin}} \in [0, 10]$ MeV. $E_{\text{dep}} = E_{\text{kin}} + 1.022$ MeV.
2. **Testing dataset:**
   - subsets with discrete kinetic energies;
   - 0 MeV, 0.1 MeV, 0.3 MeV, 0.6 MeV, 1 MeV, 2 MeV, ..., 10 MeV;
   - uniform spatial distribution;
   - each subset contains about 100 thousand events.

Aggregated features

For energy reconstruction, we use aggregated information from the whole array of PMTs as features for models. Their full set is as follows:

1. `AccumCharge` — the accumulated charge on fired PMTs;
2. `nPMTs` — the total number of fired PMTs;
3. Coordinates of the center of charge:

$$(x_{\text{cc}}, y_{\text{cc}}, z_{\text{cc}}) = \vec{r}_{\text{cc}} = \frac{\sum_{i=1}^{N_{\text{PMTs}}} \vec{r}_{\text{PMT}_i} \cdot n_{\text{p.e.},i}}{\sum_{i=1}^{N_{\text{PMTs}}} n_{\text{p.e.},i}}$$

   and its radial component: $R_{\text{cc}} = |\vec{r}_{\text{cc}}|$

4. Coordinates of the center of FHT:

$$(x_{\text{cht}}, y_{\text{cht}}, z_{\text{cht}}) = \vec{r}_{\text{cht}} = \frac{1}{\sum_{i=1}^{N_{\text{PMTs}}} \frac{1}{t_{\text{ht},i}+c}} \sum_{i=1}^{N_{\text{PMTs}}} \frac{\vec{r}_{\text{PMT}_i}}{t_{\text{ht},i}+c},$$

   and its radial component: $R_{\text{cht}} = |\vec{r}_{\text{cht}}|$

5. $\gamma_z^{\text{cc}} = \frac{z_{\text{cc}}}{\sqrt{x_{\text{cc}}^2+y_{\text{cc}}^2}}$;
6. $\gamma_y^{\text{cc}} = \frac{y_{\text{cc}}}{\sqrt{x_{\text{cc}}^2+z_{\text{cc}}^2}}$;
7. $\gamma_x^{\text{cc}} = \frac{x_{\text{cc}}}{\sqrt{z_{\text{cc}}^2+y_{\text{cc}}^2}}$;
8. $\theta_{\text{cc}} = \arctan\frac{\sqrt{x_{\text{cc}}^2+y_{\text{cc}}^2}}{z_{\text{cc}}}$;
9. $\phi_{\text{cc}} = \arctan\frac{y_{\text{cc}}}{x_{\text{cc}}}$;
10. $J_{\text{cc}} = R_{\text{cc}}^2 \cdot \sin\theta_{\text{cc}}$;
11. $\rho_{\text{cc}} = \sqrt{x_{\text{cc}}^2 + y_{\text{cc}}^2}$;
12. with 7 similar features for the components of the center of FHT.
13. Percentiles of FHT and charge distributions:
    - $\{\text{ht}_{2\%}, \text{ht}_{5\%}, \text{ht}_{10\%}, \text{ht}_{15\%}, \dots, \text{ht}_{90\%}, \text{ht}_{95\%}\}$
    - $\{\text{pe}_{2\%}, \text{pe}_{5\%}, \text{pe}_{10\%}, \text{pe}_{15\%}, \dots, \text{pe}_{90\%}, \text{pe}_{95\%}\}$
14. Differences between percentiles for FHT:
    - $\{\text{ht}_{5\%-2\%}, \text{ht}_{10\%-5\%}, \dots, \text{ht}_{95\%-90\%}\}$
15. Moments for FHT and charge distributions:
    - $\{\text{ht}_{\text{mean}}, \text{ht}_{\text{std}}, \text{ht}_{\text{skew}}, \text{ht}_{\text{kurtosis}}\}$
    - $\{\text{pe}_{\text{mean}}, \text{pe}_{\text{std}}, \text{pe}_{\text{skew}}, \text{pe}_{\text{kurtosis}}\}$

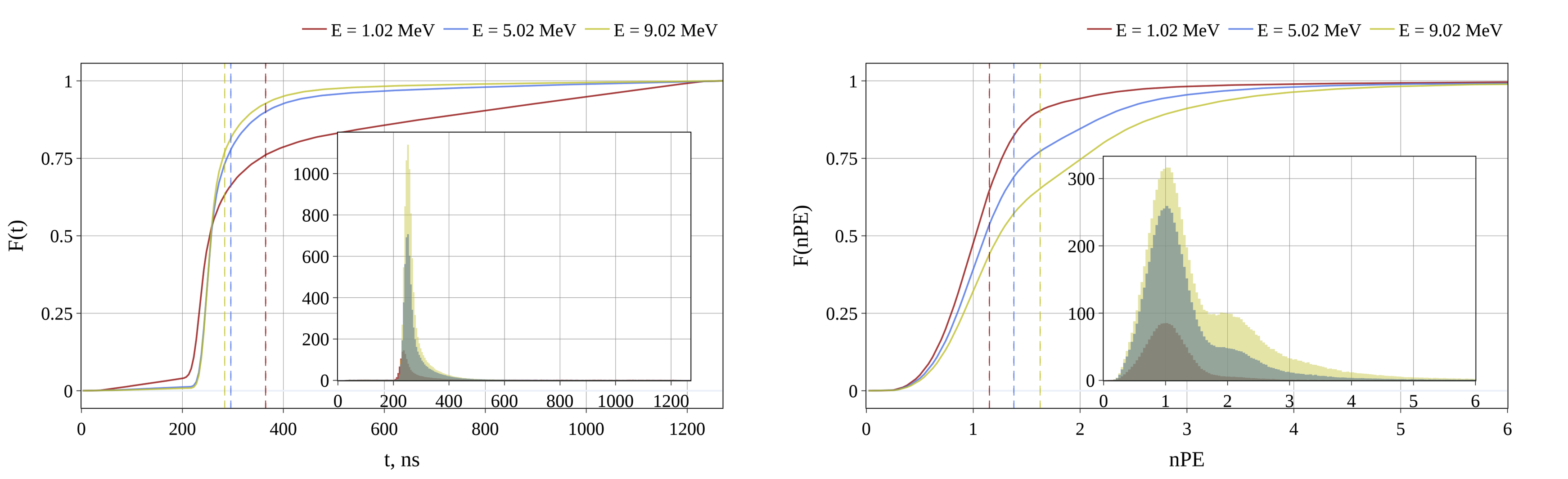

Examples of cumulative distribution functions and probability density functions for FHT (left) and charge (right) distributions. $R \simeq 0$ m, E_{kin} varied. Dashes lines illustrate mean values.

Models description

Fully Connected Deep Neural Network (**FCDNN**):

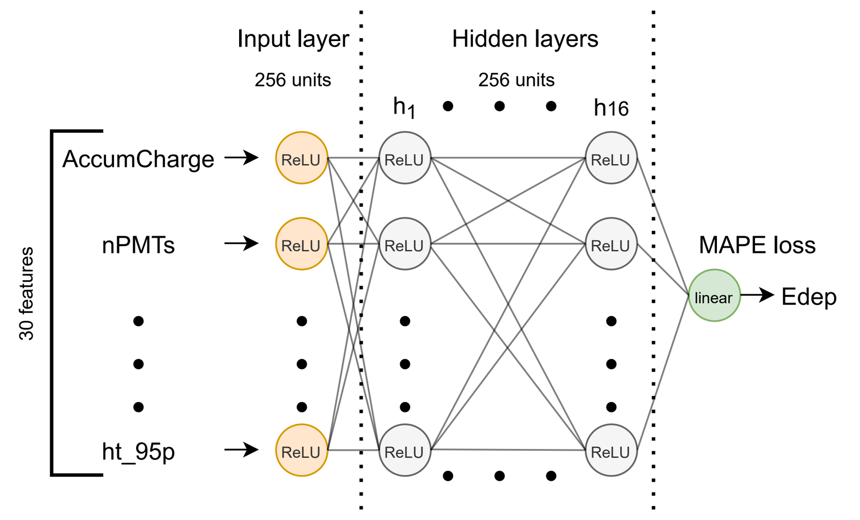

- Optimization of the hyperparameters using BayesianOptimization;
- Training with early stopping;
- Validation dataset: 400k events;
- Selected features:
  1. `AccumCharge`
  2. `nPMTs`
  3. R_{cc}
  4. R_{cht}
  5. ρ_{cc}
  6. ρ_{cht}
  7. pe_{mean}
  8. pe_{std}
  9. pe_{skew}
  10. $\text{pe}_{\text{kurtosis}}$
  11. Percentiles of FHT distribution: $\{\text{ht}_{2\%}, \text{ht}_{5\%}, \text{ht}_{10\%}, \text{ht}_{15\%}, \dots, \text{ht}_{90\%}, \text{ht}_{95\%}\}$.

Boosted Decision Trees (**BDT**) from XGBoost:
- Optimized set of features:
  1. `AccumCharge`
  2. R_{cht}
  3. z_{cc}
  4. pe_{std}
  5. `nPMTs`
  6. $\text{ht}_{\text{kurtosis}}$
  7. $\text{ht}_{25\%-20\%}$
  8. R_{cc}
  9. $\text{ht}_{5\%-2\%}$
  10. pe_{mean}
  11. J_{cht}
  12. ϕ_{cc}
  13. $\text{ht}_{35\%-30\%}$
  14. $\text{ht}_{20\%-15\%}$
  15. $\text{pe}_{35\%}$
  16. $\text{ht}_{30\%-25\%}$
- Optimized hyperparameters (using Grid Search):
  1. The maximum depth of the tree: 10;
  2. Number of trees in the ensemble: $\simeq$300;
  3. Learning rate: 0.08.

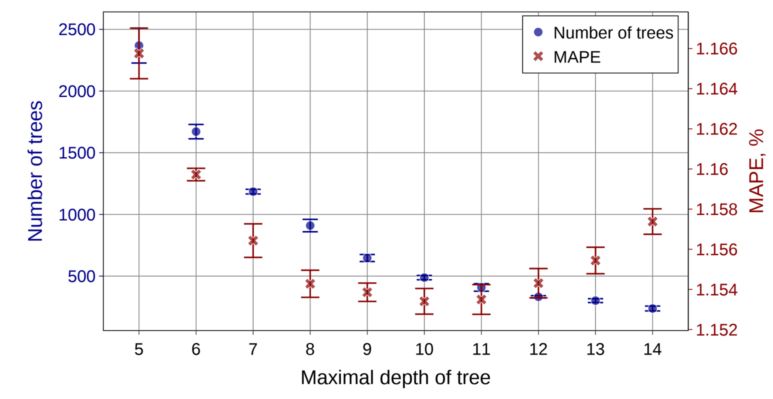

Calibration sources

JUNO has an extensive calibration program: multiple radioactive sources and background processes are planned to be used. We consider three calibration sources, listed in the following table:

Source	Type	Radiation
^{241}Am$-^{13}$C	γ	neutron + 6.13 MeV
^{60}Co	γ	1.173 + 1.333 MeV
^{68}Ge	e^+	annihilation 0.511 + 0.511 MeV

There is an additional bias, caused by the different event topology for gamma sources as opposed to positrons in the training dataset, which was corrected using values predicted by the models on pure gamma events.

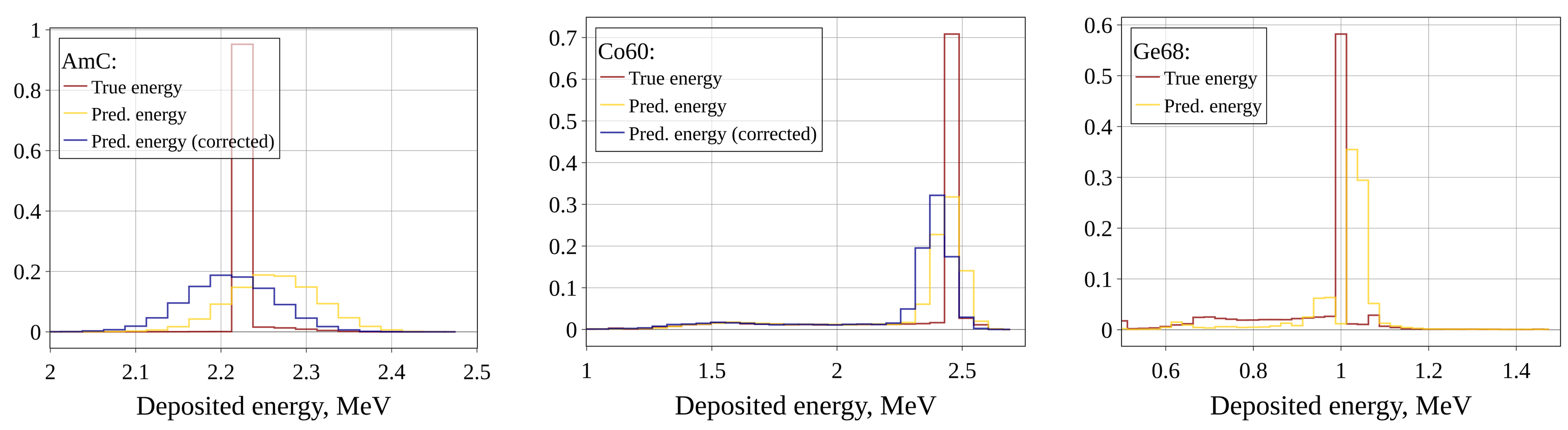

Distributions of true deposited energy and predicted energy, using the BDT model, for calibration sources.

The agreement between the expected source spectra and the spectra reconstructed from the real calibration data will indicate the correctness of the algorithms' prediction.

Results

Metrics:
1. Defined by a Gaussian fit of the $E_{\text{predicted}} - E_{\text{dep}}$ distributions;
2. *Resolution*: σ/E_{dep}, where σ — standard deviation of the fit;
3. *Bias* μ/E_{dep}, where μ — mean of the fit.

Parameterization:

$$\frac{\sigma}{E_{\text{dep}}} = \sqrt{\left(\frac{a}{\sqrt{E_{\text{dep}}}}\right)^2 + b^2 + \left(\frac{c}{E_{\text{dep}}}\right)^2}$$

The JUNO requirement to the determination of neutrino mass ordering could be translated into a convenient requirement on an effective resolution $\tilde{a}$ as:

$$\tilde{a} \equiv \sqrt{(a)^2 + (1.6 \times b)^2 + \left(\frac{c}{1.6}\right)^2} \leq 3\%$$

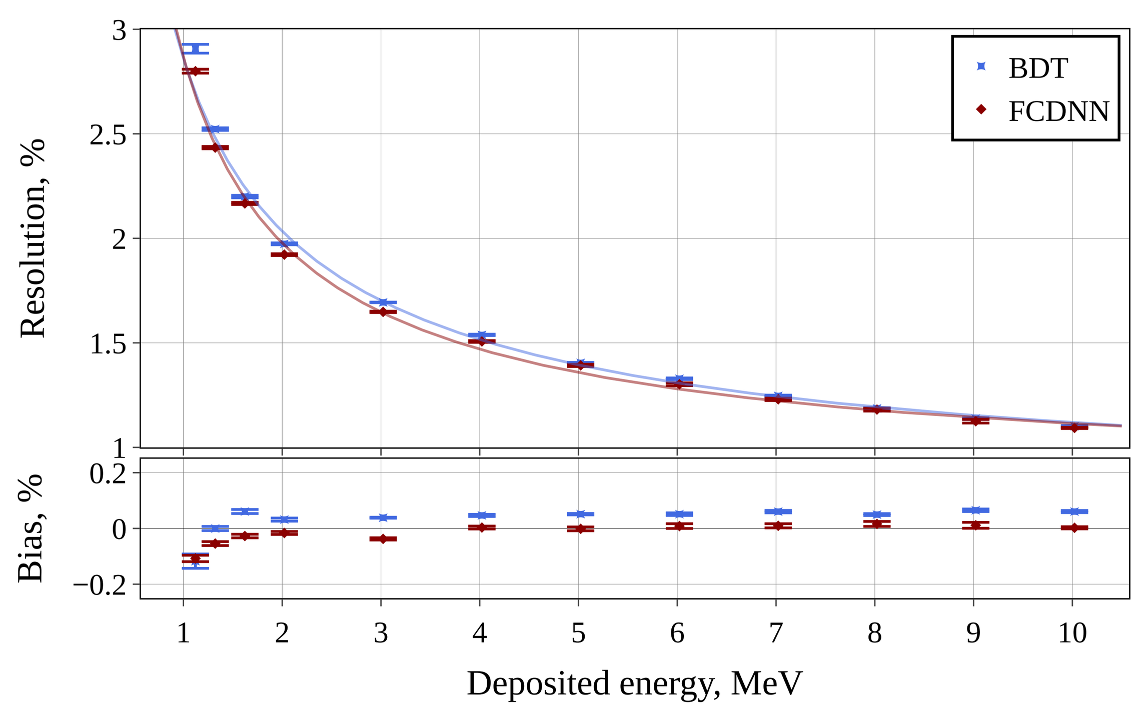

Model	$a \pm \Delta a$	$b \pm \Delta b$	$c \pm \Delta c$	$\tilde{a} \pm \Delta\tilde{a}$
BDT	2.573 ± 0.097	0.763 ± 0.045	0.990 ± 0.394	2.914 ± 0.016
FCDNN	2.316 ± 0.139	0.827 ± 0.054	1.474 ± 0.285	2.822 ± 0.027

Summary

Machine learning approaches (FCDNN and BDT) using aggregated features:
- required $\tilde{a} \leq 3\%$ achieved;
- great computation speed;
- considered three calibration sources for the future evaluation of the models on the real data.

References

[1] F. An *et al.*, *Neutrino Physics with JUNO*, J. Phys. G **43** (2016) no.3, 030401.

[2] A. Abusleme *et al.* [JUNO Collaboration], *JUNO Physics and Detector*, Prog. Part. Nucl. Phys. **123**, 103927 (2022).

[3] Z. Qian, *et al.*, *Vertex and energy reconstruction in JUNO with machine learning methods*, Nucl. Instrum. Meth. A **1010** (2021), 165527.

[4] A. Gavrikov, F. Ratnikov, *The use of Boosted Decision Trees for Energy Reconstruction in JUNO experiment*, EPJ Web Conf. **251** (2021), 03014.

Acknowledgments

We are immensely grateful to Yury Malyshkin for his invaluable contribution to this work. We also are very thankful to JUNO collaborators, who contributed to the development and validation of the JUNO simulation software.